Wetting of Regularly Structured Gold Surfaces

Mamdouh E. Abdelsalam,[†] Philip N. Bartlett,*[,†] Timothy Kelf,[‡] and Jeremy Baumberg[‡]

School of Chemistry and School of Physics and Astronomy, University of Southampton, Southampton SO17 1BJ, United Kingdom

Received October 14, 2004. In Final Form: November 22, 2004

In this study we report results for a systematic study of the wetting of structured gold surfaces formed by electrodeposition through monolayer templates of close-packed uniform submicrometer spheres. Removal of the template after deposition leaves a regular hexagonal array of sphere segment pores where the depth of the pores and, thus, the topography of the surface are controlled by the thickness of gold deposited through the template. We find that, as the thickness of the porous film increases up to the radius of the pores, the apparent contact angle for water on the surface increases from 70° on the flat surface to more that 130°, and then with increasing thickness above the radius of the pores the apparent contact angle decreases back toward 70°. We show that these changes in the apparent contact angle agree with the model of Cassie and Baxter for nonwetted surfaces even though the gold itself is hydrophilic. We also show that the apparent contact angle is independent of the diameter of the pores over the range 400−800 nm. This is the first reported example showing the change of a hydrophilic surface ($\theta < 90°$) into a hydrophobic surface ($\theta^* > 90°$) purely by control of the surface topography. The role of the pore shape and size in stabilizing the nonwetting (Cassie−Baxter) droplet on the surface is discussed.

Introduction

The wetting of solid surfaces is an important property that is controlled by both the surface energy and the geometrical microstructure of the surface.[1−5] The wettability of a surface is characterized by the contact angle, that is, the angle made between the water/air and water/solid interfaces at the three-phase boundary. Contact angle measurements are widely used to characterize the surfaces of materials[6] and surface treatments widely used to manipulate the contact angle to either increase or reduce the wetting of surfaces. Surfaces with contact angles for water of greater than 150° (superhydrophobic surfaces) have attracted much attention because of their potential practical applications[7,8] as self-cleaning surfaces and as low flow resistance coatings in microfluidic systems.[9−11] Both surface roughness and surface energy affect hydrophobicity. Thus, fractal structures have been prepared to increase surface roughness and, hence, enhance the hydrophobicity of the solid surface[12] while other experimental studies[10,13] have demonstrated that surfaces with well-ordered microstructures on the scale from a few to a hundred micrometers can also produce hydrophobic surfaces provided that the ratio of the liquid solid contact area to the overall projected contact area is small. However, so far there has been only a limited number of studies on how surface shapes and dimensions enhance surface hydrophobicity, and almost all of these have been restricted to surfaces structured on the micrometer scale and prepared by photolithographic techniques.[14,15]

Similar nanostructures are found in nature[16−18] where, for example, the striking blue color of the *Morpho sulkowskyi* butterfly originates from light diffraction and scattering produced by the ordered microstructure of its scales.[19] As well as affecting coloration, the same microstructure plays an important role in self-cleaning;[20] for the butterfly the nanostructure enhances the hydrophobicity of its wings and allows droplets of water to be dispersed more easily, carrying away with them any dust or particluates from the wing.

We recently reported[21,22] a simple technique for the preparation of ordered macroporous metal films with regular arrays of submicrometer spherical segment holes. These metal films are prepared by electrochemical reduction of metal complex ions dissolved in aqueous solution within the interstitial spaces between polystyrene latex spheres assembled on gold or indium tin oxide surfaces. The latex sphere templates are then removed by dissolving in tetrahydrofuran (THF) to leave a porous metal film with regular cavities filled with air (an inverse opal structure). Electrochemical deposition has a number of

[†] School of Physics and Astronomy, University of Southampton.
[‡] School of Chemistry, University of Southampton.

(1) Chen, W.; Fadeev, A. Y.; Hsieh, M. C.; Oner, D.; Youngblood, J.; McCarthy, T. J. *Langmuir* **1999**, *15*, 3395−3399.
(2) Gau, H.; Herminghaus, S.; Lenz, P.; Lipowsky, R. *Science* **1999**, *283*, 46−49.
(3) Lenz, P. *Adv. Mater.* **1999**, *11*, 1531−1534.
(4) Yoo, D.; Shiratori, S. S.; Rubner, M. F. *Macromolecules* **1998**, *31*, 4309−4318.
(5) Öner, D.; McCarthy, T. J. *Langmuir* **2000**, *16*, 7777−7782.
(6) Mittal, K. L. *Contact angle, wettability and adhesion*; VSP: Utrecht, The Netherlands, 1993.
(7) Miwa, M.; Nakajima, A.; Fujishima, A.; Hashimoto, K.; Watanabe, T. *Langmuir* **2000**, *16*, 5754−5760.
(8) Sun, R.; Nakajima, A.; Fujishima, A.; Watanabe, T.; Hashimoto, K. *J. Phys. Chem. B* **2001**, *105*, 1984−1990.
(9) Nakajima, A.; Fujishima, A.; Hashimoto, K.; Watanabe, T. *Adv. Mater.* **1999**, *11*, 1365−1368.
(10) Yoshimitsu, Z.; Nanajima, A.; Watanabe, T.; Hashimoto, K. *Langmuir* **2002**, *18*, 5818−5822.
(11) Patankar, N. A. *Langmuir* **2003**, *19*, 1249.
(12) Hazlett, R. D. J. *J. Colloid Interface Sci.* **1990**, *137*, 527−533.
(13) Bico, J.; Marzolin, C.; Quere, D. *Europhys. Lett.* **1999**, *47*, 220.
(14) Krupenkin, T. N.; Taylor, J. A.; Schneider, T. M.; Yang, S. *Langmuir* **2004**, *20*, 3824−3827.
(15) Shiu, J.-Y.; Kuo, C.-W.; Chen, P.; Mou, C.-Y. *Chem. Mater.* **2004**, *16*, 561−564.
(16) Kasukawa, H.; Oshima, N.; Fujii, R. *Zool. Sci.* **1987**, *4*, 243−258.
(17) Barthlott, W.; Neinhuis, C. *Planta* **1997**, *202*, 1−8.
(18) Patankar, N. A. *Langmuir* **2004**, *20*, 8209−8213.
(19) Ghiradella, H. *Appl. Opt.* **1991**, *30*, 3492−3500.
(20) Bergeron, V.; Quere, D. *Phys. World* **2001**, *14*, 2.
(21) Bartlett, P. N.; Baumberg, J. J.; Coyle, S.; Abdelsalam, M. E. *J. Chem. Soc., Faraday Discuss.* **2003**, *125*, 117−132.
(22) Bartlett, P. N.; Baumberg, J. J.; Birkin, P. R.; Ghanem, M. A.; Netti, M. C. *Chem. Mater.* **2002**, *14*, 2199−2208.

10.1021/la047468q CCC: $30.25
Published on Web 01/21/2005

significant advantages in this application. It gives a high density of deposited material with no shrinkage of the material when the template is removed. It can also be used to prepare a wide range of materials, and it allows fine control over the thickness of the final macroporous film through control of the total charge passed to deposit the film. In this paper we use templated electrochemical deposition through arrays of polystyrene spheres to produce gold films of controllable structure and investigate the relationship between the morphology of the sample and the wetting of the surface.

Experimental Section

Chemicals and Materials. Templates were made from monodisperse polystyrene latex spheres (Duke Scientific Corp., 1 wt % solution in water, coefficient of variation in diameter 1.3%). Before use, the suspensions were homogenized by successive, gentle inversions for a couple of minutes followed by sonication for 30 s.

All solvents and chemicals were of reagent quality and were used without further purification. Gold was deposited from a cyanide-free gold plating solution containing 7.07 g dm^{-3} gold (Tech. Gold 25, Technic, Inc., Cranston, RI) and 2-propanol, cysteamine, and ethanol were obtained from Aldrich. THF was obtained from Fisher Chemicals. All solutions were freshly prepared using reagent-grade water (18 MΩ·cm) from a Whatman RO80 system coupled to a Whatman "Still Plus" system.

Evaporated gold electrodes used as substrates were prepared by depositing 10 nm of chromium, followed by 200 nm of gold onto 1-mm-thick glass microscope slides. These gold substrates were thoroughly cleaned before use by sonication in deionized water for 30 min and sonication in 2-propanol for 90 min, then rinsed with deionized water, and dried under a stream of argon (BOC Gases). Cysteamine was self-assembled onto the gold electrodes by immersing the freshly cleaned substrate in a 10 mmol dm^{-3} ethanolic solution of cysteamine at room temperature for several days.

Assembly of the Colloidal Templates. Deposition of the colloidal templates was carried out in a thin layer cell (2 cm × 1.5 cm) made up of the cysteamine-coated gold electrode and a clean, uncoated microscope coverglass held 100 μm apart by a spacer cut from Parafilm (Pechiney Plastic Packaging, Inc.). The space between the two plates was filled with the aqueous 1 wt % suspension of polystyrene latex spheres. The filled thin layer cell was held vertically in an incubator (model LMS series 1) to control the rate of evaporation from the cell. After drying the templates are robust, adhere well to the gold substrates, and are opalescent in appearance. There was no evidence for resuspension of the latex particles when placed in contact with the electroplating solutions.

Electrochemical Deposition of Gold. Gold was deposited using a conventional three-electrode cell controlled by an Autolab PGSTAT30. The template-coated gold substrate was used as the working electrode with a large-area platinum gauze counter electrode and a homemade saturated calomel reference electrode (SCE). Gold was deposited under potentiostatic conditions at −0.95 V vs SCE and 25 °C. After deposition the samples were soaked in THF for 2 h to remove the polystyrene template. A Philips XL30 ESEM was used to image both the polystyrene templates and the macroporous metal films.

Contact Angle Measurement. Contact angles were determined using a purpose-built arrangement assembled on a vibrationally isolated platform. Measurements were made in a sealed glass chamber at 100% humidity. The sample was illuminated with a cold light source (Schott KL1500) and observed through an optical window in the side of the cell using a microscope. A 5-μL water drop was placed on the surface of the substrate, and the apparent contact angle, θ^*, was measured using a microscope equipped with a goniometer. All reported contact angles are the average of at least five measurements taken at different locations on the substrate and have a maximum error of ±3°.

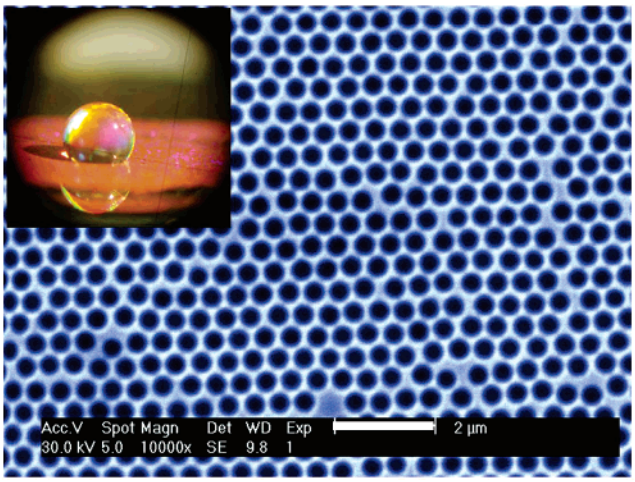

Figure 1. (a) SEM image of a gold film electrodeposited through a 500-nm-diameter polystyrene template; the inset shows an optical image for a 5-μL drop of water resting on the top of the film, $\theta^* = 131°$.

Results and Discussion

All the macroporous gold films produced by electrochemical deposition through the assembled polystyrene templates were strongly adherent to the surface of the gold substrate and highly reflective in appearance. Figure 1 shows a typical scanning electron microscopy (SEM) image of a templated gold film 170-nm thick grown through a template made up of a monolayer of 500-nm-diameter polystyrene spheres. The micrograph shows that the spherical segment voids left in the gold films after the removal of the polystyrene spheres have smooth and uniform mouths and are arranged in an ordered, hexagonal, close-packed array as expected from the structure of the original template. The individual ordered domains of hexagonal close-packed pores are of the order of 1 mm in size as determined by SEM and by laser diffraction studies. The center-to-center distance measured for the pores in the film shown in Figure 1 and for similar SEM images of other films is the same as the diameter of the polystyrene spheres used to prepare the template: the diameter of the spherical segment voids within the gold film is directly determined by the diameter of the polystyrene spheres used to form the template.

The wetting of the macroporous gold films was studied by measuring the advancing contact angle of a water drop on the top of the substrate. The inset in Figure 1 shows an optical image of a 5-μL water drop on the same gold film. The water drop shows readily visible diffractive colors ranging from blue to red, depending on the angle of observation, clearly visible when illuminated from above with white light. This is indicative of the presence of a highly ordered pore structure within the films with a pore diameter in the range of the wavelength of visible light. For the film shown in Figure 1 the contact angle was 131°. This compares to a contact angle of only 70° for the unmodified evaporated gold substrate and shows that the surface has become significantly more hydrophobic because of the nanostructure. The film consists of a hexagonal array of air-filled pores (the darker areas in Figure 1) in the gold film. The hydrophobic behavior of the film can be understood by the fact that the water is in contact with a heterogeneous surface and is supported on the gold regions with air trapped in the cavities in between. The submicrometer size, the concave internal curvature, and the sharp lip of the pores pin the drop on the top of the

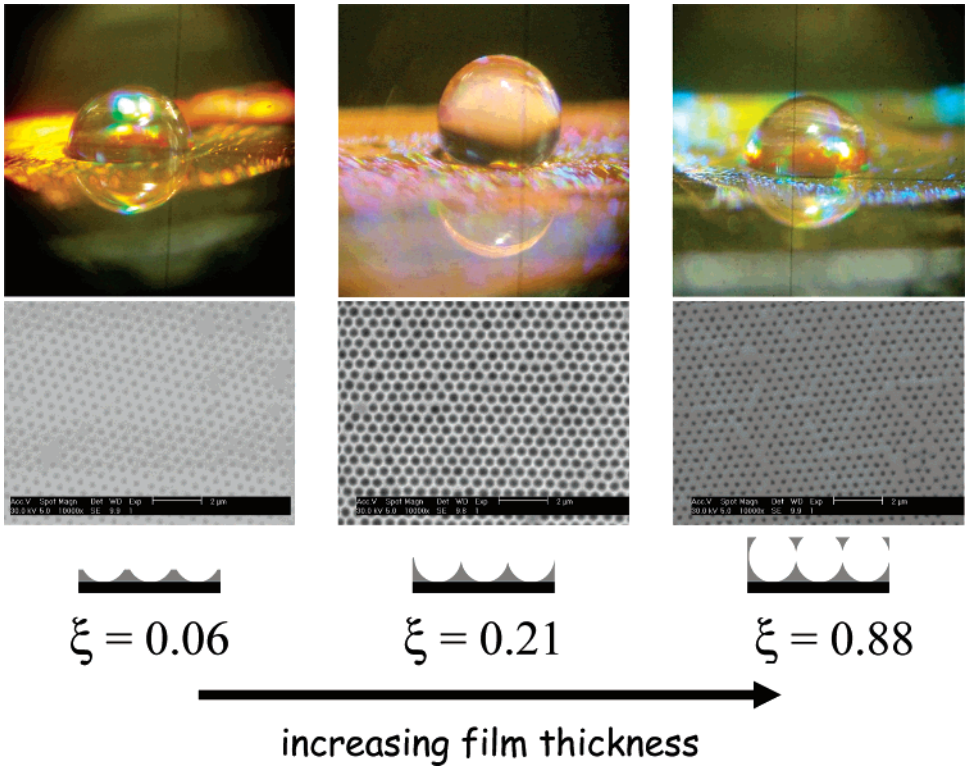

Figure 2. Optical images of 5-μL drops of water on gold macroporous films of different thicknesses are shown in the top panels, and SEM images of the corresponding surfaces are shown directly below. In each case the scale bar is 2 μm. The dimensionless thickness of each film, ξ, is given at the bottom together with a cartoon representation of the film cross-section.

film. The drops are stable on top of the mesoporous films, and the contact angle values do not change over a period of 5 h.

To understand the hydrophobic behavior of the nanostructured film we studied the variation of the apparent contact angle with film thickness and pore diameter. There are two well-established models, attributed to Wenzel[23] and Cassie and Baxter,[24] which are used to describe the wetting of rough surfaces. In Wenzel's formulation, it is assumed that the liquid fills up the rough surface, therefore, forming a fully wetted contact. The apparent water contact angle, θ^*, is then given by

$$\cos \theta^* = \phi \cos \theta \tag{1}$$

where ϕ is the roughness factor (the ratio of total surface area to the projected area in the horizontal plane) and θ is the contact angle measured on the flat surface. In the approach of Cassie and Baxter, it is assumed that the liquid forms a line of contact on the rough surface with air trapped below the contact line so that the liquid at the interface contacts both the solid and the air. The apparent contact angle can then be formulated as

$$\cos \theta^* = f_1 \cos \theta - f_2 \tag{2}$$

where f_1 is the fraction of the surface area made up of the solid and f_2 is the fraction of the surface made up of the air-filled voids; thus, $f_1 + f_2 = 1$. The statistical mechanical basis of these two equations has been examined by Swain and Lipowsky.[25]

Wenzel's equation predicts that the apparent water contact angle on hydrophilic surfaces ($\theta < 90°$), such as gold for which θ is 70°, will decrease because of surface roughness due to the increase of the total surface area ($\phi > 1$). This is the opposite of what we find experimentally.

To apply the model of Cassie and Baxter to our data we need to know the fraction of the surface area which is made up by the voids (f_2). On the basis of the geometry of the structure the void fraction of the surface is related to the film thickness, t, by

$$f_2 = \pi/2\sqrt{3}[1 - (1 - 2\xi)^2] \tag{3}$$

where ξ is the ratio of the film thickness to the diameter of the original template spheres. Film thicknesses were estimated using the radius of the pore mouth measured in SEM and the known radius of the template spheres. From simple trigonometry the thickness is given by

$$t = r \pm (r^2 - r_{\text{pore}}{}^2)^{1/2} \tag{4}$$

where t is the film thickness, r is the radius of the template sphere, and r_{pore} is the radius of the pore mouth. The choice of sign for the term in brackets depends on whether the film is thicker or thinner than the radius of the template sphere.

To test the Cassie–Baxter model the apparent contact angle for water droplets was measured for nanostructured gold films of different thicknesses and for films made by deposition through polystyrene templates assembled from spheres of different sizes. Figure 2 shows photographs of 5-μL water drops on three nanostructured gold films of various thicknesses together with cross-sectional sketches of the film geometry and scanning electron micrographs of the film surfaces. All of the films were made using templates of a monolayer of 500-nm-diameter polystyrene spheres. Note that because we used templates consisting of a monolayer of polystyrene spheres the mouths of the pores are nearly circular at all thicknesses and there is

(23) Wenzel, R. N. *Ind. Eng. Chem.* **1936**, *28*, 988–994.
(24) Cassie, A. B. D.; Baxter, S. *Trans. Faraday. Soc.* **1944**, *40*, 546–551.
(25) Swain, P. S.; Lipowsky, R. *Langmuir* **1998**, *14*, 6772–6780.

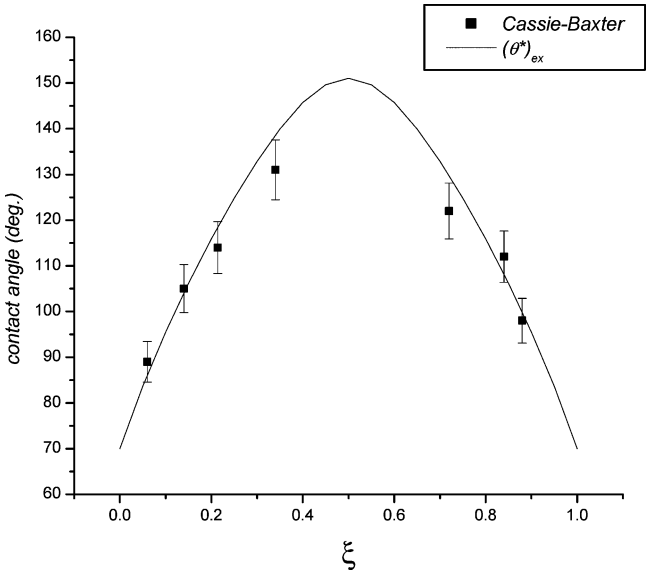

Figure 3. Effect of the dimensionless film thickness ξ (the film thickness divided by the pore diameter) on the contact angle for macroporous gold films. The films were electrodeposited through monolayer templates of 500-nm-diameter polystyrene spheres and grown to various thicknesses.

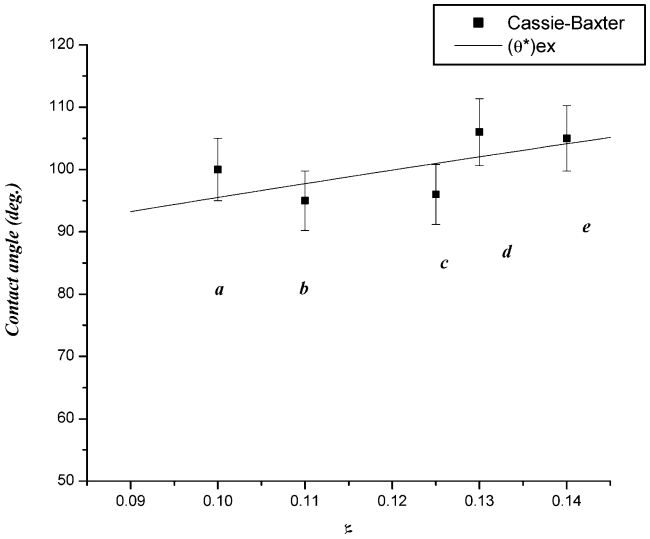

Figure 4. Influence of the sphere diameter on the contact angle for gold macroporous films. (a) $\xi = 0.1$, sphere diameter = 700 nm. (b) $\xi = 0.11$, sphere diameter = 800 nm. (c) $\xi = 0.125$, sphere diameter = 400 nm. (d) $\xi = 0.13$, sphere diameter = 600 nm. (e) $\xi = 0.14$, sphere diameter = 500 nm.

no blocking effect from a second layer of template spheres.[21] Using a monolayer template in this way simplifies the structure of the final film and allows accurate measurement of the pore mouth diameter. From the photographs it is clear that the wettability of the films changes as the film thickness and, hence, the void fraction of the surface change. For the samples in the figure the contact angles were 89, 114, and 98° for films with ξ of 0.06, 0.21, and 0.88 and with surface void fractions, f_2, of 0.21, 0.61, and 0.38, respectively. The contact angles measured for the films shown in Figure 2 together with results for other films are plotted against ξ in Figure 3. For film thicknesses up to half the template sphere diameter ($\xi < 1/2$) the contact angle increases as the film gets thicker; as the film gets thicker the diameter of the mouths of the pores increases and the surface void fraction of the area under the water drop increases, and as a result, the drops sit on more air than solid and the film becomes more hydrophobic. For film thicknesses in the range from half a sphere diameter up to one sphere diameter ($1/2 < \xi < 1$) the contact angle decreases as the film thickness increases; now the mouths of the pores decrease in diameter and, consequently, the surface void fraction decreases. The results were compared to the predictions from the model of Cassie and Baxter calculated using the measured value for the contact angle on the flat gold surface. This gives the solid line plotted in Figure 3; clearly there is good agreement between experiment and theory.

We also measured the apparent water contact angle for several nanostructured gold films prepared using template spheres of different sizes in the range 400−800 nm. In this case the films were grown to a thickness corresponding to ξ of approximately 0.12. A plot of the contact angle against ξ is shown in Figure 4 together with the curve calculated using the Cassie−Baxter model. Again there is good agreement. In this case the contact angle does not change much, although the center-to-center separation of the cavities changes.

The majority of previous experimental studies of the effects of surface topography on wetting at fabricated surfaces have used pillar geometries[10,13−15,26,27] rather than arrays of pores. A notable exception is the work of Gu et al.[28] who investigated the wetting of a fluoroalkylsilane coated silica inverse opal. They also found a significant increase in water contact angle on the structure (from 100 to 155°) although in this case they did not make quantitative comparison with theory or any systematic study of the effect of surface topography or pore size on the wettability.

An interesting feature of the data reported here is that we start with a hydrophilic surface ($\theta < 90°$) and by changing the surface topography on the submicrometer scale convert this to a hydrophobic surface ($\theta^* > 90°$). To the best of our knowledge this is the first reported example of this. According to accepted theory[29] one should expect surfaces which are hydrophilic to show Wenzel behavior and not Cassie−Baxter; consequently, one expects the apparent contact angle to decrease with increasing surface roughness, not to increase and go above 90°. The transition between Cassie−Baxter and Wenzel behavior has been discussed by Patankar[11,30] and by Lafuma and Quere.[31] According to Patankar's analysis[11] there will be an energy barrier between the two possible states, Cassie−Baxter or Wenzel, of the droplet on the rough surface but the one with the lower apparent contact angle will be the one with the lower energy. For hydrophilic surfaces ($\theta < 90°$) inspection of eqs 1 and 2 shows that this will always be the Wenzel drop because for rough surfaces $\phi > 1$ in eq 1 and $f_1 < 1$ in eq 2. Nevertheless, we see no evidence in our experiments for transition from Cassie−Baxter behavior, and we find that the drops are stable for extended periods of time (>5 h), suggesting that there is a significant barrier to transition to the Wenzel state. We suggest that the reason for this could be because of the small size and the geometry of the pores within our structure. For a spherical pore, unlike the situation for an array of pillars,

(26) Lee, W.; Jin, M.-K.; Yoo, W.-C.; Lee, J.-K. *Langmuir* **2004**, *20*, 7665−7669.
(27) He, B.; Patankar, N. A.; Lee, J. *Langmuir* **2003**, *19*, 4999−5003.
(28) Gu, Z.-Z.; Uetsuka, H.; Takahashi, K.; Nakajima, A.; Onishi, H.; Fujishima, A.; Sato, O. *Angew. Chem., Int. Ed.* **2003**, *42*, 894−897.
(29) Herminghaus, S. *Europhys. Lett.* **2000**, *52*, 165−170.
(30) Patankar, N. A. *Langmuir* **2004**, *20*, 7097.
(31) Lafuma, A.; Quere, D. *Nat. Mater.* **2003**, *2*, 457−460.

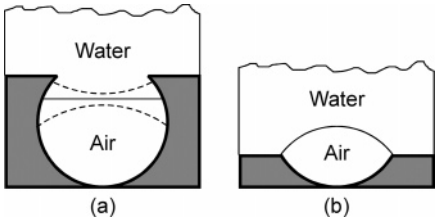

Figure 5. Wetting of spherical cavities. The solid line shows the local equilibrium position of the liquid−vapor interface. The dotted line shows the shape of the interface away from this local minimum: (a) the situation for a deep pore, (b) the situation for a shallow pore.

for a hydrophilic surface there will be some position within the pore at which, for the given contact angle θ, the liquid vapor interface will be planar (Figure 5a). This is a local energy minimum; moving away from this position in either direction requires curvature of the liquid vapor interface to maintain the local contact angle, and this curvature, according to Young's equation, raises the energy of the system. Because the spherical cavities are small (diameter < 1 μm) the increase in curvature of the interface is significant leading to a significant increase in the energy of the system. Consequently there is a significant energy barrier to overcome in going from the metastable Cassie−Baxter to the Wenzel situation. In the case where the porous film is thin so that the spherical segment cavities are not deep enough to allow the liquid to form a planar surface within the cavity we suggest that the liquid vapor interface is pinned at the mouth of the cavity (Figure 5b). This situation minimizes the curvature of the interface; again for the liquid to penetrate into the cavity the curvature is required to increase and so is energetically unfavorable. The mechanism described in Figure 5 is speculative, and further work needs to be done to investigate the pinning of drops on these surfaces.

Summary and Conclusions

From our results we conclude that the electrochemical deposition of metals through assembled templates of monodisperse polystyrene spheres is a simple and effective method to produce macroporous films of controlled thickness and pore size. The film simultaneously exhibits structural color and hydrophobicity. Controllable variations in the surface morphology can be used to systematically vary the wetting of the surface. In our experiments hydrophilic gold surfaces ($\theta = 70°$) were changed into hydrophobic surfaces ($\theta^* > 90°$) by controlling the nanostructure. Our results cannot be explained by the model of Wenzel but are in excellent agreement with the model of Cassie and Baxter for rough surfaces. It is clear that this method can be readily extended to make macroporous films from the wide range of different metals and alloys that can be deposited electrochemically from aqueous solutions.

Acknowledgment. This work was funded by EPSRC Grant GR/R54194.

LA047468Q